Interaction of Oxo-Bridged Vanadium(III) Phenanthroline and Bipyridine Dimers with DNA

Shiela J. Heater,[†] Mary W. Carrano,[†] Douglas Rains,[†] Ronald B. Walter,[†] David Ji,[‡] Quing Yan,[‡] Roman S. Czernuszewicz,[‡] and Carl J. Carrano*[,†]

Department of Chemistry and Biochemistry, Southwest Texas State University, San Marcos, Texas 78666, and Department of Chemistry, University of Houston, Houston, Texas 77204

Received April 14, 2000

Cationic μ-oxo V(III) dimers of the type $[V_2OL_4Cl_2]^{2+}$ (L = 1,10-phenanthroline, 3,4,7,8-tetramethyl-1,10-phenanthroline, 4,7-diphenyl-1,10-phenanthroline, or 2,2′-bipyridine) are shown to interact very strongly with DNA and to lead ultimately to its degradation. Spectroscopic binding studies, electrophoreses, DNA melting temperature experiments, and other tests on the parent 1,10-phenthroline complex all yield results consistent with tight binding. However, the exact nature of the binding—i.e., intercalative, groove binding, electrostatic, or covalent—remains unclear. Resonance Raman spectroscopy is found to be a powerful method for studying the interaction of these μ-oxo V(III) dimers with DNA and shows that in frozen aqueous solution, the parent complex $[V_2O(phen)_4Cl_2]^{2+}$ undergoes initial aquation, followed by the reaction of the aquated species with the DNA. Once the V(III) dimer is bound to the DNA, redox takes place, leading to the formation of alkaline-sensitive lesions. Hydrogen peroxide is implicated as a partner in this redox event, based on the effects of the enzymes SOD and catalase.

Introduction

The interaction of metal ions with nucleic acids and their constituents has been an area of intense interest to both inorganic chemists and biochemists, and metal complexes, most notably those of Pt(II), have found their way into the pharmaceutical armamentarium as potent antitumor drugs.[1] The fact that some naturally occurring antitumor antibiotics such as bleomycin require metal cofactors for their biological activity (which involves DNA strand scission) has also prompted the examination of metal complexes for their endonuclease activity.[2] This has stimulated the development of metal complexes that cleave DNA, with the objective of obtaining new pharmaceutical agents, artificial restriction endonucleases, and probes for DNA−protein contacts and DNA structure.[3] Systems based on copper, iron, ruthenium, rhodium, cobalt, manganese, nickel, gold, and chromium have all been investigated for DNA cleavage activity, with the most attention focused on the mid to late transition elements and comparatively little attention paid to the earlier members of the series.[4−12] Among the latter, vanadium, with its three biologically accessible oxidation states (III, IV, and V), has begun to be recognized as having important biological roles.[13−15] The lack of studies based on the interaction of vanadium with DNA is surprising in view of the reports that two other anticancer agents derived from vanadium—i.e., vanadium-substituted bleomycin and $[(phen)VO(H_2O)_2]^{2+}$—cause DNA strand scission.[16,17] The few studies that have appeared have generally been restricted to cases where vanadium is in its highest oxidation state (V).[18−20]

While the interaction of monometallic complexes with nucleic acids has been widely studied, dimetallic systems have rarely been examined despite the fact that such sites are commonly used by nature in phosphate-hydrolyzing enzymes and DNA polymerases.[21,22] Dimetallic complexes might be expected to bind strongly to DNA via a two-point attachment, which, in turn, could lead to enhanced activity. Dinuclear Pt complexes and carboxylate-bridged dinuclear Rh, Ru, and Re, for example, have been reported to possess significant carcinostatic activity.[1] Also, the interaction of dinuclear Fe and Ni complexes with

* Corresponding author.
[†] Southwest Texas State University.
[‡] University of Houston.

(1) See: Orvig, C., Abrams, M. J., Eds. *Chem. Rev.* **1999**, *99*.
(2) Stubbe, J.; Kozavich, J. W. *Chem. Rev.* **1987**, *87*, 1107.
(3) See: Bashkin, J. K., Ed. *Chem. Rev.* **1998**, *98*.
(4) Yam, V.; Choi, S.; Lo, K.; Dung, W.; Kona, R. *J. Chem. Soc., Chem. Commun*. **1994**, 2379.
(5) Gupta, N.; Grover, N.; Neyhart, K. G. A.; Singh, P.; Thorp, H. *Inorg. Chem*. **1993**, *32*, 310.
(6) Hegg, E. L.; Burstyn, J. N. *Inorg. Chem*. **1996**, *35*, 7474.
(7) Sigman, D. S. *Acc. Chem. Res.* **1986**, *19*, 180.
(8) Gravert, D. J.; Griffin, J. H. *Inorg. Chem*. **1996**, *35*, 4837.
(9) Barton, J. K.; Rapheal, A. *Proc. Natl. Acad. Sci. U.S.A.* **1985**, *82*, 6460.
(10) Morrow, J. R.; Kolaser, K. A. *Inorg. Chim. Acta* **1992**, *195*, 245.
(11) Cheng, C.; Rokita, S. E.; Burrows, C. J. *Angew. Chem., Int. Ed. Engl*. **1993**, *32*, 277.
(12) Kumar, C. V.; Tan, W. B.; Betts, P. W. *J. Inorg. Biochem*. **1997**, *68*, 177.
(13) *Metal Ions in Biological Systems*; Sigel, H., Sigel, A., Eds.; Marcel Dekker: New York, 1995; Vol. 31.
(14) Rehder, D. *Angew. Chem., Int. Ed. Engl*. **1991**, *30*, 148.
(15) Butler, A.; Carrano, C. J. *Coord. Chem. Rev.* **1991**, *109*, 61.
(16) Kuwahara, J.; Suzuki, T.; Sugiura, Y. *Biochem. Biophys. Res. Commun.* **1985**, *129*, 368.
(17) Sakurai, H.; Tamura, H.; Okatani, K. *Biochem. Biophys. Res. Commun.* **1995**, *206*, 133.
(18) Sakurai, H.; Nakai, M.; Miki, T.; Tsuchiya, K.; Takada, J.; Matsushita, R. *Biochem. Biophys. Res. Commun.* **1992**, *189*, 1090.
(19) Kwong, D. W.; Chan, O. Y.; Wong, R. N.; Musser, S. M.; Vaca, L.; Chan, S. I. *Inorg. Chem*. **1997**, *36*, 1276.
(20) Hiort, C.; Goodisman, J.; Dabrowiak, J. C. *Biochemistry* **1996**, *35*, 12354.
(21) Sträter, N.; Lipscomb, W. N.; Klabunde, T.; Krebs, B. *Angew. Chem., Int. Ed. Engl*. **1996**, *35*, 2024.
(22) Steinhagen, H.; Helmchen, G. *Angew. Chem., Int. Ed. Engl*. **1996**, *35*, 2339.
(23) Schnaith, L. M.; Hanson, R. S.; Que, L. *Proc. Natl. Acad. Sci. U.S.A.* **1994**, *91*, 569.

10.1021/ic000389r CCC: $19.00
Published on Web 08/04/2000

DNA has been reported,[23,24] with the Fe complex being particularly active at promoting the cleavage of double-stranded DNA.

The μ-oxo V(III) dimers are potentially interesting candidate dinuclear complexes. We were attracted to them because we felt that such dimers might adapt themselves to the DNA groove conformation to maximize secondary interactions. In previous studies, we have shown that in the absence of any cobridging ligands, the V−O−V unit is quite flexible, but if there are no external influences, it adopts the expected strictly linear geometry where π bonding between the bridging oxygen and the vanadium(III) is maximized. However, weak forces such as $\pi-\pi$ stacking interactions can lead to a slight bending of the V−O−V unit.[25] Still stronger interactions such as hydrogen bonding can lead to even further distortions from linearity, as does the addition of cobridging ligands.[26−28]

We report here our results with several such compounds of the type $[V_2OL_4Cl_2]^{2+}$ (L = 2,2′-bipyridine or substituted *o*-phenanthroline) and show that not only do they exhibit different reactivity patterns with DNA than with the corresponding monomers, they do so in the absence of any externally added agents, such as hydrogen peroxide. A preliminary account of portions of this work has already appeared.[25]

Experimental Section

Physical Methods. The resonance Raman spectra were obtained with discrete lines (568.2 and 676.4 nm) from a Coherent K-2 Kr^+ ion laser. Room-temperature spectra were measured from the solution (H_2O or methanol) in a spinning NMR tube[29] or the KCl pellet in a solid-state spinning Raman cell,[30] using a scanning Raman instrument described elsewhere.[31] Low-temperature (77 K) spectra were obtained using a liquid N_2 Raman cell.[32] The typical laser powers were 100−200 mW, with 4−6 cm^{-1} slit widths. Multiple scans (3−5) were averaged to improve the signal-to-noise ratio. Raman data manipulation (signal averaging and spectral deconvolution) was performed using an IBM PC version of LabCalc software (Galactic Industries, Inc.). The CURVEFIT routine was used to deconvolute overlapped peaks into Gaussian curves.

Materials. Vanadium complexes were synthesized as previously described.[25] Unless otherwise noted, all syntheses were performed under an inert atmosphere of nitrogen or argon with a Vacuum Atmospheres drybox or through standard Schlenk techniques. Aqueous solutions of the vanadium compounds were prepared by dissolving an appropriate amount of the vanadium compound in sterilized, deoxygenated water. All vanadium solutions were prepared fresh and used immediately or kept at 0 °C to minimize oxidation.

Plasmids pUB110 (4500 bp, 3 MDa) and pBR322 (4363 bp, 2.9 MDa) were purchased from Sigma and dissolved in 20 μL of sterile distilled water, resulting in a final buffer concentration of 1 mM Tris-HCl at pH 7.5 and 1 mM NaCl. The DNA solutions were stored in 10 μL aliquots at −20 °C. The oligonucleotide corresponding to the TAR sequence was prepared by IDT (Integrated DNA Technology, Ames, IA) and purified by gel electrophoresis.[33]

Plasmid DNA was assayed using a 1% agarose gel run for 3 h at 100 V constant voltage (or 18 h at 25 V), and the DNA bands were detected after being stained for 30 min in a 0.5 μg/mL ethidium bromide solution in 1× TBE buffer. Following destaining for 30 min in water, the gels were visualized on a Kodak Digital Science IS440CF system and analyzed using Kodak Digital Science 1D Image analysis software. Values for supercoiled plasmid DNA were corrected by a factor of 1.3, based on estimates of lowered binding affinity of ethidium bromide for the supercoiled DNA form.[34]

Plasmid Cleavage Reactions. Aqueous solutions of the vanadium compounds were prepared as described above and mixed with 0.5 μg of plasmid DNA (pUB110 or pBR322) in 16 mM Tris-acetate at pH 8.4. The final volumes were brought to 10 μL with sterile distilled water and incubated for 5−60 min at 37 °C. The reactions were quenched by the addition of 2 μL of loading buffer (0.5% bromophenol blue, 10 mM EDTA, and 50% glycerol). Anaerobic reactions were carried out under nitrogen with the use of a glovebag. Base-sensitive lesions were revealed by adding piperidine to the samples to a final concentration of 0.1 M and by heating the mixture at 90 °C for 30 min.

Oligonucleotide Cleavage Reactions. One microgram of 31-mer was end-labeled via a 20 min incubation at 37 °C with T4 kinase (Gibco) and [^{32}P]dATP (NEN). Following the incubation, the sample was ethanol-precipitated, and the pelleted DNA was resuspended in TAE buffer without EDTA. The resulting 5′-^{32}P-labeled 31-mer was then reacted with the vanadium dimer at various concentrations for 30 min. After reaction of the mixtures, each reaction tube was split: half was immediately quenched with formamide loading buffer, while the other half was treated with 0.1 M piperidine for 30 min at 90 °C. Following the removal of the piperidine and the addition of loading buffer, approximately 40 000 counts of each fraction were loaded onto a 20% acrylamide sequencing gel for analysis via autoradiography.

Plasmid End-Labeling Reactions. The vanadium-treated DNA was ethanol-precipitated in $^1/_{10}$ volume of 3 M sodium acetate and 2.5 volumes of ethanol at −80 °C for 10 min. The precipitated DNA was pelleted at 13000*g* for 15 min and dried under vacuum. The pelleted DNA was resuspended in TAE buffer, and the concentration of the solution was determined by UV absorbance. Duplicate samples were treated with DNA polymerase I in the presence of [^{32}P]dCTP, followed by incubation at 37 °C for 20 min. Duplicate samples of the vanadium-treated DNA were incubated with T4 kinase in the presence of [^{32}P]-dATP, followed by incubation at 37 °C for 20 min. Following the incubations, the samples were ethanol-precipitated, and the pelleted DNA was resuspended in 20 μL of TAE buffer. Ten-microliter aliquots of the samples were loaded onto the wells of a 1% (w/v) agarose gel and electrophoresed for 17 h at constant 33 V. The gel was photographed and dried for autoradiography. The gel was exposed to Kodak XAR X-ray film for 4 h at room temperature and for 8 h at −80 °C. Positive controls were prepared by the exposure of supercoiled pUB110 to DNase I.

$[V_2OL_4Cl_2]^{2+}$ Binding to Calf Thymus DNA. Concentrated stock solutions of calf thymus (CT) DNA were prepared in CT DNA buffer (50 mM NaCl, 5 mM Tris-HCl, pH 7.1). The concentration of the DNA solution in nucleotide phosphate [NP] was determined by UV absorbance at 260 nm (ϵ_{260} = 6600 M^{-1} cm^{-1}).[35] Stock DNA solutions were stored at 4 °C for no longer than one week. Solutions of the complex (100 μM) were prepared in deoxygenated CT DNA buffer, mixed with increasing concentrations of CT DNA, and incubated for 5 min at 0 °C. The absorbance values were plotted against R (R = [DNA]/[[$V_2OL_4Cl_2$]$^{2+}$]). The intrinsic association constant K_a for the interaction of $[V_2OL_4Cl_2]^{2+}$ with CT DNA was calculated from the absorption titration data using the following equation:

$$[\mathrm{DNA}]/(\epsilon_f - \epsilon_a) = [\mathrm{DNA}]/(\epsilon_f - \epsilon_b) + 1/K_a(\epsilon_f - \epsilon_b)$$

(24) Kesicki, E. A.; DeRosch, M. A.; Freeman, L. H.; Walden, C. L.; Harvey, D. F.; Trogler, W. C. *Inorg. Chem.* **1993**, *32*, 5851.
(25) Otieno, T.; Bond, M. R.; Mokry, L. M.; Walter, R. B.; Carrano, C. J. *J. Chem. Soc., Chem. Commun.* **1996**, 37.
(26) Czernuszewicz, R. S.; Yan, Q.; Bond, M. R.; Carrano, C. J. *Inorg. Chem.* **1994**, *33*, 6116.
(27) Czernuszewicz, R. S.; Bond, M. R.; Dave, B. C.; Mohan, M.; Verastgue, R.; Carrano, C. J. *Inorg. Chem.* **1995**, *34*, 5857.
(28) Carrano, C. J.; Verastgue, R.; Bond, M. R. *Inorg. Chem.* **1993**, *32*, 3589.
(29) Czernuszewicz, R. S. *Appl. Spectrosc.* **1986**, *40*, 571.
(30) Walters, M. A. *Appl. Spectrosc.* **1983**, *37*, 299−301.
(31) Czernuszewicz, R. S.; Johnson, M. K. *Appl. Spectrosc.* **1983**, *37*, 297.
(32) Czernuszewicz, R. S. In *Methods in Molecular Biology*; Jones, C., Mulloy, B., Thomas, A. H., Eds.; Humana Press Inc.: Totawa, NJ, 1993; Vol. 17, pp 345−374.
(33) Carter, P. J.; Breiner, K. M.; Thorp, H. H. *Biochemistry* **1998**, *37*, 13736.
(34) Hertzberg, R. P.; Dervan, P. B. *Biochemistry* **1984**, *23*, 3934.
(35) Reichmann, M. E.; Rice, S. A.; Thomas, C. A.; Doty, P. *J. Am. Chem. Soc.* **1954**, *76*, 3047.

Table 1. Selected Bond Lengths (Å) and Angles (deg) for $[V_2OCl_2(phen)_4]Cl_2$ and $[V_2OCl_2(bipy)_4]Cl_2$

	phen[a]	bipy[b]
V−Cl	2.361(2)	2.381(2)
V−O	1.784(1)	1.787(1)
$V-N_{cis}$	2.132(4)	2.124(12)
$V-N_{trans}$	2.194(5)	2.178(6)
V−O−V	169.6(3)	173.5(2)

[a] Data from ref 25. [b] Data from ref 46.

where $\epsilon_a = A_{obsd}/[(V_2OL_4Cl_2)^{2+}]$ and ϵ_f and ϵ_b correspond to the molar absorbtivities of $[V_2OL_4Cl_2]^{2+}$ in the free and fully bound forms, respectively. $[DNA]/(\epsilon_f - \epsilon_a)$ was plotted versus [DNA], and the association constant K_a was obtained from the ratio of the slope to the intercept.

DNA Melting Curve Determination. Calf thymus DNA (96 μM) in 5 mM Tris-HCl at pH 7.1 and 50 mM NaCl was mixed with 5 μM phenanthroline dimer and placed in a water-jacketed quartz cuvette. The samples were heated with a temperature-controlled water bath, and the absorbance at 260 nm was monitored with the Beckman DU-7400 spectrophotometer. Melting curves were constructed by plotting relative absorbance versus temperature.

Results

Solid-State and Solution Structures. Since our preliminary account of the structures of both the V(III) phenanthroline dimer and the V(IV) monomer, which are both similar to their bipyridine analogues, has already appeared and the details are on deposit at the Cambridge Structural Database, they will not be repeated here. However, a few pertinent bond lengths and angles are included in Table 1. The slightly smaller bridge angle and smaller intermetallic distance in the phenanthroline dimer relative to the bipyridine analogue likely result from the increased π stacking interaction in the former. This highlights the most striking feature of the secondary structure of the dimer, the proximity of two of the phenanthroline rings coordinated to opposite metals (Figure 1). These rings are nearly parallel to one another and separated by 3.45 Å, with a twist angle of about 22.5° between them. In principle, this interplanar spacing is almost perfect for the intercalation of both phenanthroline rings between the base pairs of B-DNA.

Resonance Raman (RR) spectroscopy has been very useful in defining the solution structures of oxo-bridged V(III) dimers due to the presence of strong μ-O → V(III) charge-transfer transitions in the visible region and its sensitivity to even small changes in the V−O−V bridging angle.[26,27,36−39] Compared in Figure 2 are the solid-state and solution RR spectra of $[V_2OCl_2(phen)_4]Cl_2$ obtained at room temperature in the 100−1500 cm^{-1} region with 676.4 nm excitation from the samples (a) dispersed in a pressed KCl pellet, (b) dissolved in methanol, and (c) dissolved in water. The RR spectrum of $[V_2OCl_2(phen)_4]Cl_2$ in methanol (Figure 2b) is nearly identical to that in the solid state (Figure 2a), each spectrum showing four bands characteristic of the V−O−V bridge at very similar frequencies, ~377, 673, 753, and 1336 cm^{-1}. The 377 and 673 cm^{-1} bands in both spectra are identified as the in-phase (symmetric) and out-of-phase (antisymmetric) V−O−V stretching vibrations, ν_s(VOV) and ν_{as}(VOV), respectively. The other two bands (~753 and 1336 cm^{-1}), which occur at nearly twice the frequencies of the 377 and 673 cm^{-1} fundamentals, arise from the first overtones of ν_s(VOV) and ν_{as}(VOV), $2\nu_s$(VOV) and $2\nu_{as}$(VOV), respectively. These assignments have been confirmed with RR experiments involving isotope substitution of the μ-oxo group with μ-^{18}O and with normal-mode analysis calculations.[39] The nearly identical frequencies of these vibrational modes indicate that the structure of the (Cl)V−O−V(Cl) core has not been changed in the MeOH solution.

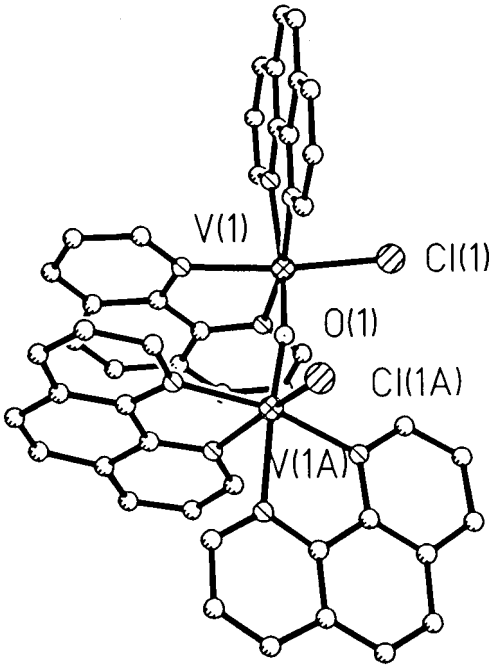

Figure 1. Structure of $[V_2OCl_2(phen)_4]^{2+}$ showing the stacking of the phenanthroline rings and the cis disposition of the chloride ligands.

The RR spectrum of $[V_2OCl_2(phen)_4]Cl_2$ changes, however, when H_2O is added to the MeOH solution; the ν_s(VOV) band at 377 cm^{-1} loses its intensity, and a new broad band appears at 367 cm^{-1}. At the same time, the ν_{as}(VOV) (~673 cm^{-1}) and $2\nu_{as}$(VOV) (~1336 cm^{-1}) bands upshift by ~10 and ~20 cm^{-1} (data not shown). In pure H_2O, ν_s(VOV), ν_{as}(VOV), and $2\nu_{as}$(VOV) shift to 366, 695, and 1380 cm^{-1}, respectively, and the $2\nu_s$(VOV) overtone moves underneath the phenanthroline ligand band at 734 cm^{-1} (Figure 2c), implying that the (Cl)V−O−V(Cl) core geometry has been altered by the aqueous environment. The structural change may involve the opening of the V−O−V angle (which is ~168° in solid state),[25] or it may involve a V−O−V bridge that has assumed a nonsymmetrical geometry through hydrolysis of a terminal chloride ligand. Such structural changes would be consistent with the observed pattern of both the ν_s(VOV) and the ν_{as}(VOV) frequencies in H_2O, i.e., lower frequency for ν_s(VOV) but higher frequency for ν_{as}(VOV) in the aqueous state than in the solid state and MeOH.

Additional environmental effects on the V−O−V stretches were observed upon freezing the aqueous solution of $[V_2OCl_2(phen)_4]Cl_2$ at liquid-N_2 temperature. This is illustrated in Figure 3, which shows the frozen solution RR spectra obtained at ~77 K in the 100−1500 cm^{-1} region with excitation wavelengths of (a) 568.2 and (b) 676.4 nm. The 568.2 nm excitation spectrum exhibits two dominant bands in the ν_s(VOV) region, at 366 and 379 cm^{-1}, with only a very weak and broad feature in the ν_{as}(VOV) region, at ~690 cm^{-1} (Figure 3a). The first overtone of the 379 cm^{-1} band can also be seen at 758 cm^{-1}. In contrast, the 676.4 nm excitation gives the RR spectrum with much

(36) Kanamori, K.; Ookubo, Y.; Ino, K.; Kawai, K.; Michibata, H. *Inorg. Chem.* **1991**, *30*, 3832−3836.
(37) Kanamori, K.; Ino, K.; Maeda, K. M.; Fukagawa, M.; Kumada, J.; Eguchi, T.; Okamoto, K.-I. *Inorg. Chem.* **1994**, *33*, 5547.
(38) Czernuszewicz, R. S.; Spiro, T. G. In *Inorganic Electronic Structure and Spectroscopy*; Solomon, E. I., Lever, A. B. P., Eds.; Wiley-Interscience: New York, 1999; Vol. 1, pp 353−442.
(39) Czernuszewicz, R. S.; Yan, Q.; Ji, D.; Carrano, C. J. Manuscript in preparation.

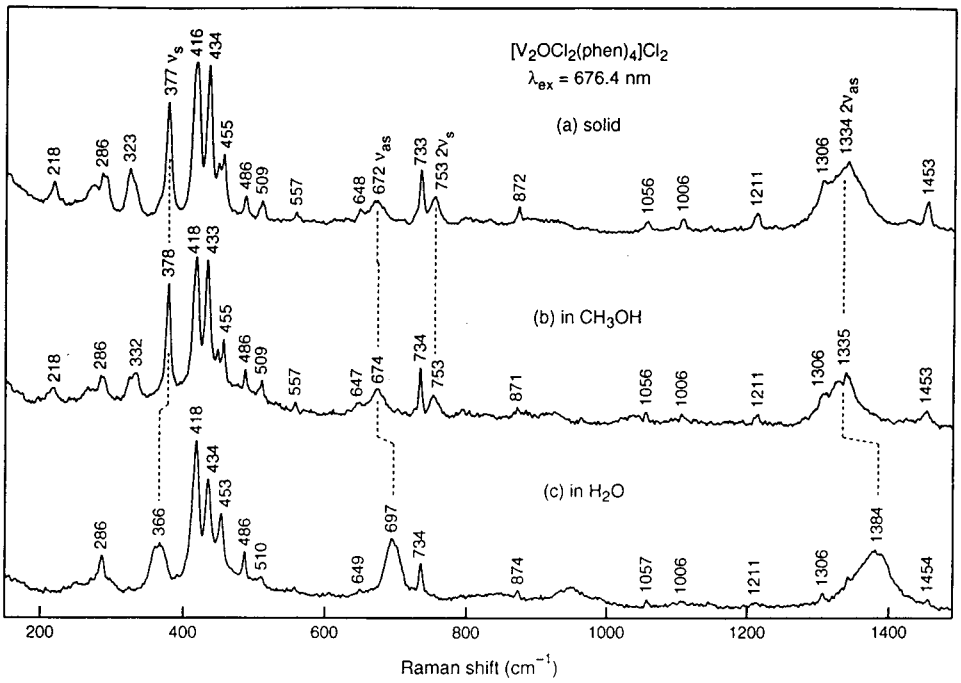

Figure 2. Room-temperature RR spectra (676.4 nm excitation) of (a) polycrystalline $[V_2OCl_2(phen)_4]Cl_2$ (KCl pellet) and its (b) aqueous and (c) methanol solutions. The V−O−V stretching vibrations are correlated.

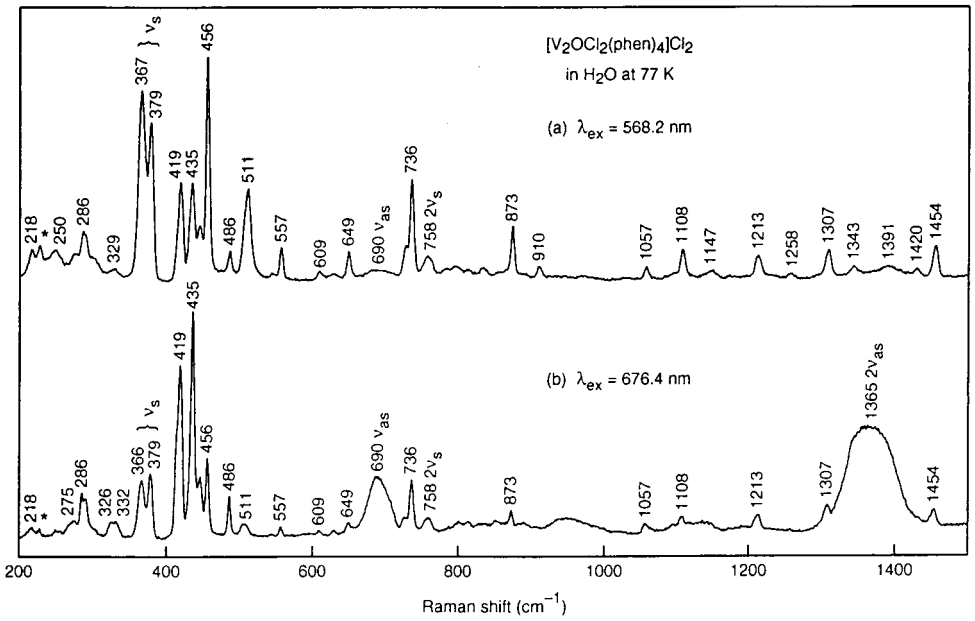

Figure 3. Low-temperature (~77 K) RR spectra of $[V_2OCl_2(phen)_4]Cl_2$ in H_2O excited at (a) 568.2 and (b) 676.4 nm. The V−O−V stretching vibrations are correlated.

weaker bands attributable to ν_s(VOV) but intense bands in the ν_{as}(VOV) and $2\nu_{as}$(VOV) regions (Figure 3b). The widths and shapes of these bands, which are centered near 690 and 1365 cm^{-1}, respectively, clearly show that they contain overlapping component bands. Spectral deconvolution of the 620−780 and 1275−1375 cm^{-1} regions into a combination of Gaussian curves (see below) has revealed ν_{as}(VOV) fundamentals at 683 and 695 cm^{-1}, $2\nu_s$(VOV) overtones at 734 and 758 cm^{-1}, and $2\nu_{as}$(VOV) overtones at 1348 and 1384 cm^{-1}. Hence, two different μ-oxo-bridged V(III) species are present in the frozen (~77 K) aqueous solution of $[V_2OCl_2(phen)_4]Cl_2$. The 367 cm^{-1} (ν_s), 734 cm^{-1} ($2\nu_s$), 695 cm^{-1} (ν_{as}), and 1384 cm^{-1} ($2\nu_{as}$) modes seen at liquid-N_2 temperature closely correspond to those observed in the room-temperature spectrum of the complex in H_2O (Figure 2c), which we believe belong to the dimer that contains aqua ligands in place of the chloride ligands.[39] The second set of V−O−V modes at 379 cm^{-1} (ν_s), 758 cm^{-1} ($2\nu_s$), 683 cm^{-1} (ν_{as}), and 1348 cm^{-1} ($2\nu_{as}$) has been observed in solid-state RR spectra at ~77 K with almost identical (within ±1 cm^{-1}) frequencies (data not shown). These bands belong to the species containing a (Cl)V−O−V(Cl) core but with a somewhat different geometry than that observed in the X-ray crystal structure and polycrystalline RR spectrum at room temperature, as judged from the significantly upshifted (10−12 cm^{-1}) ν_{as}(VOV) and $2\nu_{as}$(VOV) bands at liquid-N_2 temperature. These observations are summarized in Table 2.

Redox Activity. All the reported oxo-bridged V(III) dimers are more or less sensitive to air oxidation in solution, although they appear to be quite stable in the solid state. The major oxidation product appears to be the V(IV) monomer, [VO-

$(phen)_2Cl]^+$. The electrochemistry of the unsubstituted dimer in the aprotic solvent, acetonitrile (ACN), has already been reported by Maverick et al. (although at the time it was reported to be a hydroxo-bridged species).[40] Our results are similar with the dimer oxidizing irreversibly to monomer that then undergoes both oxidation and reduction. However, we have also examined the electrochemistry in a 1:1 mixed-solvent system containing ACN and the protic solvent methanol (MeOH). In this solvent, the redox chemistry is different and, presumably, more relevant to the situation in aqueous solution. In ACN/MeOH, the dimer undergoes two quasireversible one-electron oxidations at 515 and 816 mV, which we assign to the $V^{3+}-O-V^{4+}$ and $V^{4+}-O-V^{4+}$ dimers. Also observed is an irreversible reduction at −795 mV (with a peak height approximately twice that of the oxidation waves), which is assigned to the two-electron reduction of the dimer to the V(II) monomer

$$[Cl(phen)_2V^{III}-O-V^{III}(phen)_2Cl]^{2+} + 2e^- + 2H^+ \rightarrow 2[V^{II}(phen)_2Cl]^+ + H_2O$$

Although we assign this irreversible reduction as metal-centered, a ligand-centered reduction is also a possibility. Under the same conditions, the authentic V(IV) monomer shows no oxidation up to 1.0 V in an initial positive scan but gives an irreversible reduction at −873 mV. Scanning through the reductive wave then reveals two quasireversible product waves at 464 and 847 mV. We interpret this behavior as indicating an ECE mechanism where there is an initial two-electron reduction and protonation of the vanadyl complex to give a V(II) monomer, followed by a rapid reaction with the remaining V(IV) monomer and comproportionation to give the oxo-bridged V(III) dimer, which can in turn undergo two reversible oxidations.

$$[V^{IV}O(phen)_2Cl]^+ + 2e^- + 2H^+ \rightarrow [V^{II}(phen)_2Cl]^+ + H_2O \qquad E$$

$$[V^{II}(phen)_2Cl]^+ + [V^{IV}O(phen)_2Cl]^+ \rightarrow [Cl(phen)_2V^{III}-O-V^{III}(phen)_2Cl]^{2+} \qquad C$$

$$[Cl(phen)_2V^{III}-O-V^{III}(phen)_2Cl]^{2+} \rightarrow [Cl(phen)_2V^{III}-O-V^{IV}(phen)_2Cl]^{3+} + e^- \qquad E_1$$

$$[Cl(phen)_2V^{III}-O-V^{IV}(phen)_2Cl]^{3+} \rightarrow [Cl(phen)_2V^{IV}-O-V^{IV}(phen)_2Cl]^{4+} + e^- \qquad E_2$$

The bipyridine and substituted phenanthroline complexes show qualitatively similar behavior with only relatively small shifts in the relevant potentials. Although the oxidations of the dimer in MeOH/ACN are reversible on the CV time scale, attempted bulk electrolysis yields only the vanadyl monomer, presumably due to a relatively slow reaction of the very oxophilic $V^{IV}-O-V^{IV}$ dimer with traces of water

$$[Cl(phen)_2V^{IV}-O-V^{IV}(phen)_4Cl]^{4+} + H_2O \rightarrow 2[V^{IV}O(phen)_2Cl]^+ + 2H^+$$

Attempts to conduct electrochemical experiments in pure water were complicated by the exchange of chloride with water and/or hydroxide, leading to multiple species and complex voltammograms. Thus, we have not examined it further.

(40) Shah, S. S.; Maverick, A. W. *Inorg. Chem.* **1987**, *26*, 1559.

Table 2. V−O−V Stretching Mode Frequencies (cm^{-1}) for $[V_2OCl_2(phen)_4]Cl_2$ and Its CT DNA Adduct[a]

sample	ν_s	ν_{as}	$2\nu_s$	$2\nu_{as}$	species[b]
Room Temperature					
KCl pellet	377	672	753	1334	**A**
MeOH solution	378	674	753	1335	**A**
H_2O solution	366	697	732	1384	**B**
Liquid-N_2 Temperature					
KCl pellet	378	684	756	1348	**A′**
H_2O frozen solution	379	683	758	1348	**A′**
	367	697	734	1383	**B**
DNA precipitate	379	683	758	1349	**A′**
	372	706	743	1402	**C**

[a] ν_s and ν_{as} are the symmetric (in-phase) and antisymmetric (out-of-phase) stretching modes, respectively, of theV−O−V bridge; $2\nu_s$ and $2\nu_{as}$ are the corresponding first overtone bands. [b] Capital letters denote species with different structures of the μ-oxo divanadium bridge: **A** = parent dimer with chloro terminal ligands, **A′** = parent dimer with slightly altered bridge, **B** = dimer with aquo terminal ligands, and **C** = DNA−dimer complex.

Binding to Calf Thymus DNA. As expected from their structure, all the V(III) dimeric complexes appear to interact strongly with DNA, and the addition of aqueous solutions of the former causes the rapid precipitation of DNA. The dark-purple color of the precipitate indicated that the V(III) dimer is bound to DNA. Precipitated samples stored for up to 3 days remained purple, unlike unbound solutions of the dimer, which were completely oxidized within hours. Thus, the binding of the dimer to DNA clearly reduced its accessibility to and/or reactivity with dioxygen, suggesting a tight association. Quantitative evaluation of the binding affinity of the dimer for CT DNA utilized a spectrophotometric assay.[41] Binding of the dimer containing the unsubstituted phenanthroline to CT DNA in 50 mM NaCl and 5 mM Tris-HCl at pH 7.0 resulted in changes to the ligand-to-metal charge-transfer (LMCT) bands of the complex near 542 and 642 nm. Upon addition of CT DNA, an increase in the absorbance of the two LMCT bands, along with a small (ca. 6 nm) blue shift, is observed. The absorbance reaches a maximum at an R value (R = [DNA]/[dimer]) of approximately 3 before decreasing slightly and leveling off. Since obvious precipitation is observed at R values greater than 5, some precipitation could be occurring at values between 3 and 5, thus accounting for the small hypochromism seen over this range. An association constant can be extracted from the titration data using the method previously described.[41] The K_a calculated from the data in Figure 4 is 5.3×10^5 M^{-1}. While this value is smaller than that found for classical intercalators such as ethidium bromide under similar conditions (1.4×10^6 M^{-1} at 40 mM NaCl and 25 mM Tris-HCl),[42] it is similar to that found for several mixed-ligand ruthenium complexes (10^3−10^5 M^{-1}) thought to be behave as such.[43] However, intercalators normally display hypochromism and small red shifts upon binding to DNA, in contrast to the hyperchromism and blue shifts of the V(III) dimers. Attempts to acquire similar data for the other compounds in the series were thwarted by the rapid precipitation of DNA even at small R values.

Changes in the melting temperature of DNA in the presence of interacting compounds are well known. Thus, we have measured the T_m for CT DNA in the presence and absence of the V(III) phenanthroline dimer (Figure 5). Binding of the complex causes the T_m to increase from 68 to 76 °C. The

(41) Mhadevan, S.; Palaliandavar, M. *Inorg. Chim. Acta* **1997**, *254*, 291.
(42) Waring, M. J. *J. Mol. Biol.* **1965**, *13*, 269.
(43) Pyle, A. M.; Rehmann, J. P.; Meshoyrer, R.; Kumar, C. V.; Turro, N. J.; Barton, J. K. *J. Am. Chem. Soc.* **1989**, *111*, 3051.

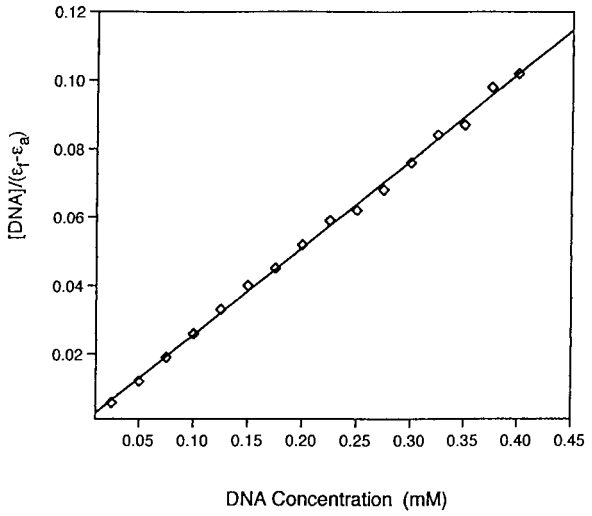

Figure 4. Plot of $[DNA]/(\epsilon_f - \epsilon_a)$ vs [DNA], where ϵ_f and ϵ_a are the molar absorbtivities for the complex in the free and bound (attached) forms, respectively. The intrinsic binding constant is calculated from these data as described in the text.

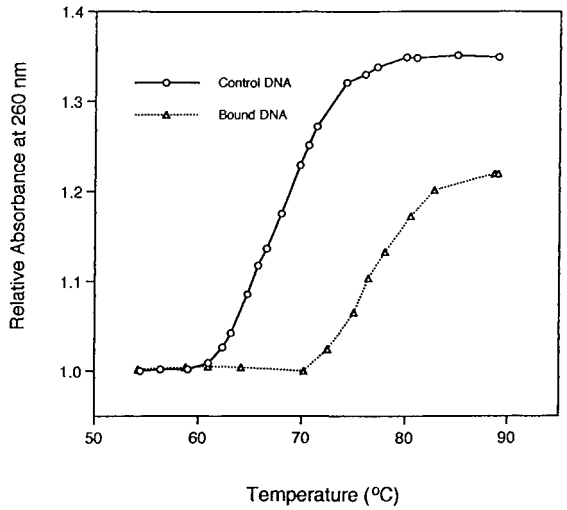

Figure 5. Melting curves for calf thymus DNA (96 μM) in the presence and absence of 5 μM $[V_2OCl_2(phen)_4]Cl_2$.

observed CT DNA hypochromism may be due to increased base stacking caused by intercalation of the complex. The increased T_m indicates a stabilization of the helix; however, this could be due to simple charge neutralization of the polyanionic phosphate backbone by the cationic vanadium complex, by intercalation, or by both.

The nature of the interaction of the vanadium(III) dimer with CT DNA was further probed by low-temperature (~77 K) RR spectroscopy of the dark-purple precipitate resulting from mixing the aqueous solutions of $[V_2OCl_2(phen)_4]Cl_2$ and CT DNA. The results are shown in Figure 6 (200−800 cm^{-1}) and Figure 7 (1000−1600 cm^{-1}), which compare the 676.4 nm excitation spectra of (a) frozen aqueous $[V_2OCl_2(phen)_4]^{2+}$ and (b) the frozen precipitate with CT DNA. The precipitated DNA has RR spectra very similar to that of the $[V_2OCl_2(phen)_4]Cl_2$ complex in frozen H_2O, except for the regions where characteristic vibrations of the V(III)−O−V(III) bridge occur. In the ν_s(VOV) region, a pair of bands at 367 and 379 cm^{-1} of the dimer in pure water (Figure 6a) collapse into an asymmetric band centered at ~374 cm^{-1} when the complex binds to DNA (Figure 6b). The yellow line excitation (568.2 nm) gives relatively stronger ν_s(VOV) RR bands (see Figure 3), and the

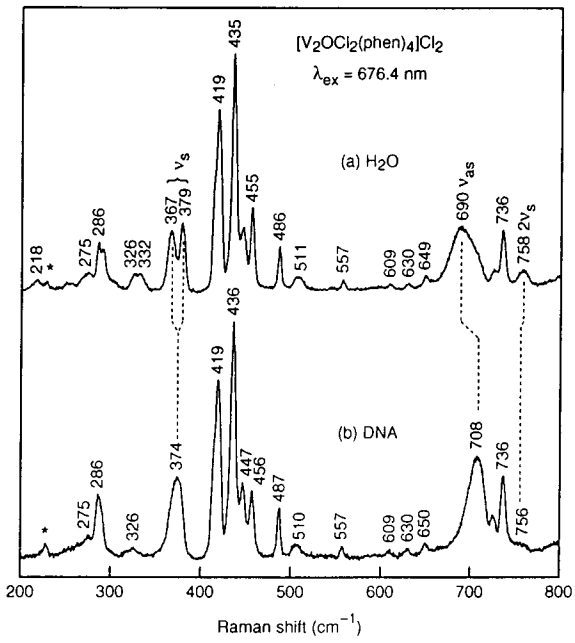

Figure 6. Comparison of the low-temperature (~77 K) RR spectra (676.4 nm excitation) in the 200−800 cm^{-1} region of (a) $[V_2OCl_2(phen)_4]Cl_2$ in H_2O and (b) its CT DNA-bound product. The V−O−V stretching vibrations are correlated.

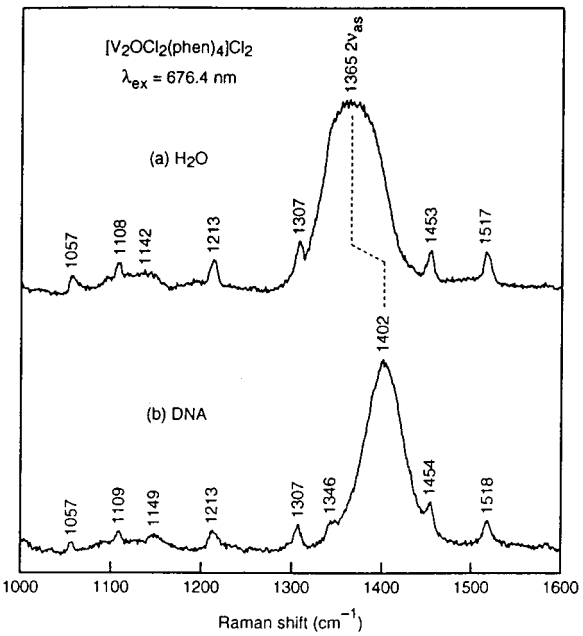

Figure 7. Comparison of the low-temperature (~77 K) RR spectra (676.4 nm excitation) in the 1000−1600 cm^{-1} region of (a) $[V_2OCl_2(phen)_4]Cl_2$ in H_2O and (b) its CT DNA-bound product. The V−O−V stretching vibrations are correlated.

~374 cm^{-1} band observed with the red line (676.4 nm) appears to better resolve into two components (~372 and ~377 cm^{-1}) in the spectrum excited at 568.2 nm (Figure 8b). Meanwhile, the $2\nu_s$(VOV) band of the $\nu_s = 379$ cm^{-1} fundamental appears to shift from 758 (H_2O) to ~756 cm^{-1} (DNA).

The more dramatic changes, however, occur among the RR bands assigned to ν_{as}(VOV) (Figure 6) and $2\nu_{as}$(VOV) (Figure 7) vibrations, which are strongly enhanced in spectra excited at 676.4 nm. Without DNA, these vibrations lead to broad and poorly shaped bands at ~690 (ν_{as}) and ~1365 cm^{-1} ($2\nu_{as}$) but produce appreciably narrower and upshifted bands in the DNA precipitate spectrum at ~708 (ν_{as}) and ~1402 cm^{-1} ($2\nu_{as}$). We

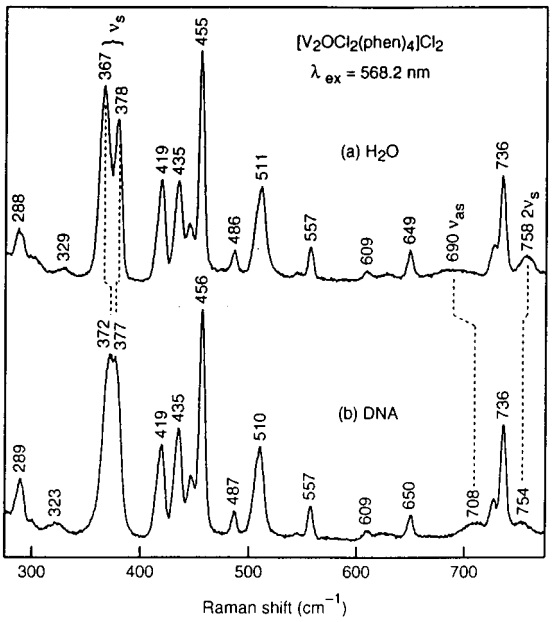

Figure 8. Comparison of the low-temperature (~77 K) RR spectra (568.2 nm excitation) in the 275−775 cm^{-1} region of (a) $[V_2OCl_2(phen)_4]Cl_2$ in H_2O and (b) its CT DNA-bound product. The V−O−V stretching vibrations are correlated.

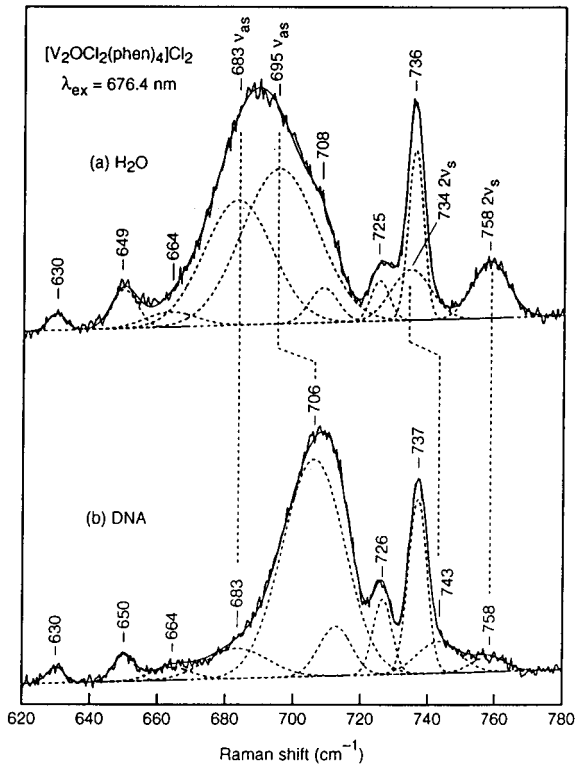

Figure 9. Structure of the ν_{as}(VOV) fundamental band of $[V_2OCl_2(phen)_4]Cl_2$ excited with 676.4 nm radiation: (a) in the frozen H_2O solution at ~77 K and (b) in the frozen CT DNA precipitate at ~77 K.

have obtained more precise positions for the ν_{as}(VOV) and $2\nu_{as}$(VOV) modes of both samples by deconvoluting overlapped peaks in these regions into a combination of Gaussian curves, as shown in Figure 9 (620−780 cm^{-1}) and Figure 10 (1275−1475 cm^{-1}). As previously mentioned, these analyses reveal that two forms of the V(III) dimer exist in the frozen H_2O solution, one characterized by the bands at 683 (ν_{as}) and 1348 cm^{-1} ($2\nu_{as}$) and another by the bands at 695 (ν_{as}) and 1383

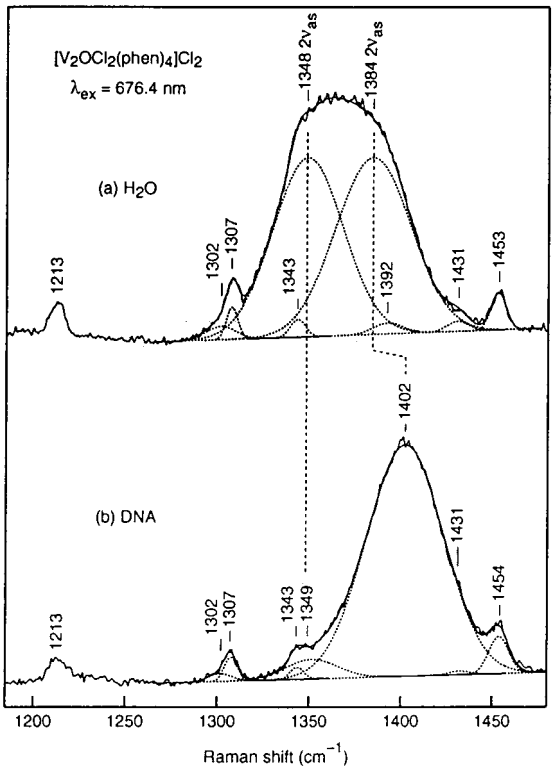

Figure 10. Structure of the $2\nu_{as}$(VOV) overtone band of $[V_2OCl_2(phen)_4]Cl_2$ excited with 676.4 nm radiation: (a) in the frozen H_2O solution at ~77 K and (b) in the frozen CT DNA precipitate at ~77 K.

cm^{-1} ($2\nu_{as}$). Small contributions from the former pair of modes are also evident in the DNA precipitate spectra at unchanged positions (Figures 9b and 10b). Since solid $[V_2OCl_2(phen)_4]Cl_2$ at ~77 K exhibits similar V−O−V stretching modes (data not shown), the 683 (ν_{as}) and 1348 cm^{-1} ($2\nu_{as}$) bands in the DNA precipitate spectrum, as well as their corresponding bands ν_s at 379 cm^{-1} and $2\nu_s$ at 758 cm^{-1}, must arise from the $[V_2OCl_2(phen)_4]^{2+}$ that remains unbound to DNA in the mother liquor solution. On the other hand, the 695 (ν_{as}) and 1383 cm^{-1} ($2\nu_{as}$) bands disappear from the deconvoluted spectra of the DNA precipitate and are replaced by a pair of dominant bands at 706 (ν_{as}) and 1402 cm^{-1} ($2\nu_{as}$). The corresponding ν_s(VOV) and $2\nu_s$(VOV) for the DNA-bound dimer modes are located at 372 and 743 cm^{-1}, respectively. Thus, in summary, the oxo-bridged vanadium(III) dimer in frozen aqueous solution is characterized by the RR bands at 367 (ν_s), 734 ($2\nu_s$), 695 (ν_{as}), and 1383 cm^{-1} ($2\nu_{as}$), which, upon the binding of the complex to DNA, shift upward to 372, 743, 706, and 1402 cm^{-1}, respectively.

Nucleolytic Activity of the Oxo-Bridged Dimers. Nucleolytic activity of the vanadium dimers was assayed by incubation with supercoiled plasmid DNA. Single-strand breaks cause unwinding to the open circular form, and double-strand cuts or numerous single-strand breaks within close proximity to each other produce linear DNA. Figure 11 indicates the relative amounts of supercoiled or closed circular (CC), open circular (OC), and linear (L) pBR322 plasmid DNA as a function of the concentration of the phenanthroline dimer. Complete conversion from CC to OC occurs at about 0.2 mM complex. Bands at concentrations above 0.3 mM display considerable broadening, and precipitation of the DNA is observed above 1.0 mM. Also notable is the concentration-dependent band retardation of the CC form. Similar experiments were performed using the bipyridine, tetramethylphenanthroline, and diphen-

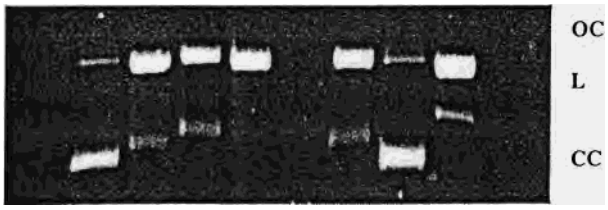

Figure 11. Cleavage of the plasmid pBR322 by $[V_2OCl_2(phen)_4]Cl_2$. Lanes 1−4 contain 0, 47, 94, and 188 μM vanadium complexes, respectively. Lane 6 contains 94 μM vanadium complex only, lane 7 contains 94 μM vanadium plus 0.5 μL of catalase, and lane 8 contains 94 μM vanadium plus 1 μL of SOD.

ylphenanthroline dimers, and the data are summarized in Table 3. The bipyridine and diphenylphenanthroline dimers were less reactive than the parent phenanthroline complex, and the tetramethylphenanthroline derivative was more reactive. However, the rapid air oxidation of the latter rendered it difficult to work with, and thus, all further studies were concentrated on the unsubstituted phenanthroline complex. Several additional experiments indicated that the reaction was completed very rapidly (within minutes) and was not markedly temperature dependent, although some slowing of the reaction at 4 °C was noted.

During longer incubations at low concentrations, the deep purple color of the dimer faded as the dimer was oxidized to the vanadyl monomer. Thus, it was necessary to determine whether the nucleolytic activity was an inherent property of the dimer or of the monomer and/or if dioxygen was a coreactant. For this, we incubated the complex with plasmid DNA under anaerobic conditions. The conditions were sufficient to suppress any obvious oxidation of the dimer as determined optically, but no effect was noted on the cleavage reaction. We also examined the reaction of aged solutions of the dimer and authentic $[VO(phen)_2Cl]^+$. These experiments show that the vanadyl monomer does in fact induce plasmid cleavage reactions at concentrations similar to that of the dimer but with two notable differences. First, very little band retardation is observed with the monomer, indicating a different interaction with the plasmid; second, there is an increased formation of linear fragments (Table 3) compared to what is seen for the dimer. When hydrogen peroxide is included in the incubation mixture, both monomer and dimer yield identical results, extensive cleavage of the plasmid DNA, resulting in large amounts of the linear form (indicating double-strand breaks). We attribute this result to the fact that in the presence of hydrogen peroxide, the V(III) dimer is rapidly converted to the V(IV) monomer (as determined spectrophotometrically), and vanadyl complexes of various types are known to yield hydroxyl radicals in the presence of excess peroxide via Fenton-type chemistry.[9,10] These observations, combined with the results of the anaerobic incubation, indicate that both the V(IV) monomer and the V(III) dimer react independently via different mechanisms to cleave plasmid DNA. More detailed studies of $[VO(phen)_2Cl]^+$ and the V(V) analogue $[VO_2(phen)_2]^+$ will be reported at a later date.

Although dioxygen itself did not appear to be important in the dimer-induced cleavage reaction, we examined the effects of radical scavengers on the reaction. The addition of known scavengers of hydroxyl radicals (either DMSO or sodium formate) had little or no effect on the reaction. These reagents effectively suppress FeEDTA-mediated cleavage reactions. Thus, diffusible hydroxyl radicals appear not to be involved in the mechanism. The SOD and catalase enzymes did, however, have significant effects (Figure 11). Catalase clearly inhibits the reaction, while SOD potentiates it. Since catalase converts hydrogen peroxide to dioxygen and water while SOD dismutes superoxide to hydrogen peroxide and dioxygen, the reactive oxygen species appears to be hydrogen peroxide.

Table 3. Relative Nucleolytic Activities of Vanadium Complexes[a]

complex	% CC	% OC	% L
$[V_2OCl_2(bipy)_4]Cl_2$	52	48	0
$[V_2OCl_2(phen)_4]Cl_2$	25	73	2
$[V_2OCl_2(Me_4phen)_4]Cl_2$	2	95	3
$[V_2OCl_2(diphenylphen)_4]Cl_2$	100	0	0
$[VOCl(phen)_2]Cl$	14	74	12

[a] DNA samples (pUB110) incubated for 30 min at 37 °C with 100 μM complex. CC = closed circular, OC = open circular, and L = linear.

Nature of the DNA Lesion. A number of experiments were undertaken to learn more about the specific nature of the damage created upon the incubation of DNA with the dimer. The nature of the termini remaining after V(III) dimer-induced nicking was investigated by enzymatic end-labeling and ligation studies. Hydrolytic cleavage is expected to result in the production of both 3′-OH and 5′-PO_4 ends, while other mechanisms produce different termini.[2,44] Following treatment with DNA polymerase I, V(III) dimer-nicked DNA was efficiently labeled with ^{32}P, indicating the presence of at least some 3′-OH ends and the absence of adducts capable of halting polymerase strand synthesis. The treatment of V(III)-nicked DNA with T4 kinase under conditions that favor phosphate exchange resulted in the efficient incorporation of ^{32}P, suggesting the presence of either free or phosphorylated 5′ ends. Although we were unable to quantitate the number of such reactive ends, in both cases, the vanadium-nicked DNA was labeled to a greater degree than hydrolytically nicked controls (DNAase). Attempts at seeing if these ends could be enzymatically linked with T4 ligase were unsuccessful due to the difficulty in preparing sufficient quantities of linear V(III)-treated plasmid DNA.

The possibility of oxidative base loss as indicated by alkaline-sensitive lesions on dimer-nicked plasmid DNA was assayed by hot piperidine treatment. This resulted in greatly increased cleavage—as manifested by a smear of small fragments upon electrophoresis of plasmid treated with dimer and then with piperidine—and indicated that base loss accompanied the reaction.

Reaction with Small (31-mer) DNA Oligomers. To gain insight into possible base sequence or secondary structure specificity, we examined the reaction of the phenanthroline dimer with a ^{32}P-end-labeled DNA 31-mer modeled after the HIV-1 TAR mRNA sequence.[33] This self-complementary oligomer contains a three-base "bulge" and a six-base "hairpin" loop. These experiments complemented and extended the results from the plasmid assay. In the absence of piperidine treatment, modest cleavage of the 31-mer was detected along with concentration-dependent band retardation and smearing of the intact oligomer on the sequencing gel (Figure 12). Careful analysis reveals the presence of "shadow bands", indicating the presence of multiple termini. The major bands comigrate with the Maxam−Gilbert sequencing bands (3′-phosphate), while the minor bands do not. After hot piperidine treatment, more extensive cleavage was evident, and the anomalous migration pattern of the intact 31-mer vanished, as did the presence of the shadow bands. All bands now comigrate with the Maxam−Gilbert ones. If SOD was included in the reaction mixture, significant cleavage was noted even prior to piperidine treatment, with extensive cleavage seen afterward. The cleavage pattern

(44) Meunier, B. *Chem. Rev.* **1992**, *92*, 1411.

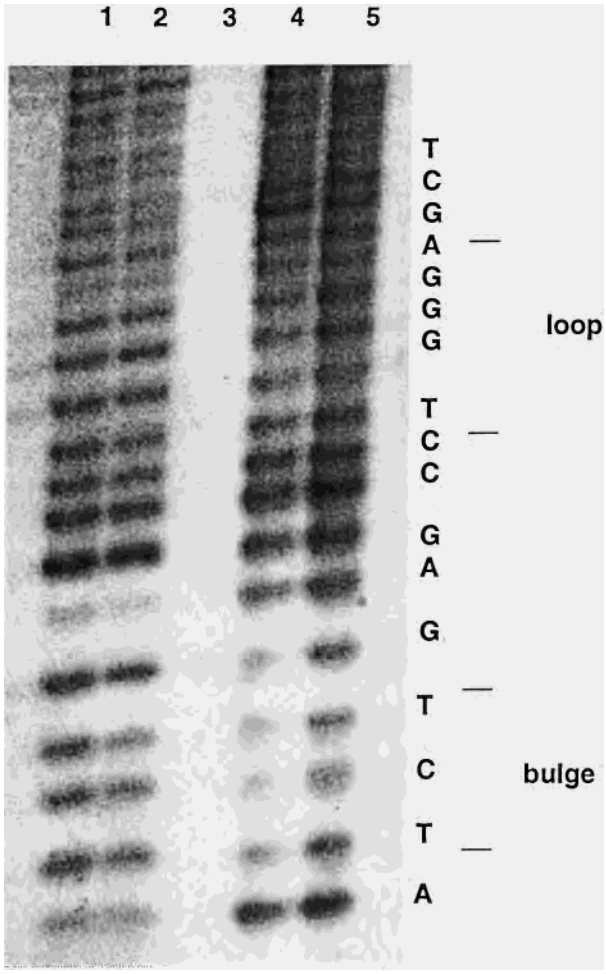

Figure 12. Autoradiogram of a polyacrylamide gel showing the reaction of 5′-^{32}P-labled 31-mer with $[V_2OCl_2(phen)_4]Cl_2$. Lanes 1 and 2 are treated with 0.67 and 1.33 mM vanadium dimer, respectively, and then with piperidine; lane 3 is blank; lanes 4 and 5 are treated with 0.67 and 1.33 mM vanadium dimer, respectively, plus 10 μL of SOD without piperidine treatment (note that in the presence of SOD, more cleavage is evident even without piperidine treatment).

was qualitatively the same with or without SOD and showed little or no sequence specificity, although some preference for the first double-stranded regions on either side of the hairpin and bulge structure was noted. In the presence of catalase, little or no cleavage was seen, with or without piperidine treatment (data not shown). The addition of excess hydrogen peroxide, which causes the oxidation of the V(III) dimer to the V(IV) monomer, gave rise to a different fragmentation pattern, confirming that the monomer and dimer both cleave DNA but by different means and/or have different specificities.

Discussion

It is clear that cationic μ-oxo dimers of V(III) interact very strongly with DNA. Indicators of this are (1) the concentration-dependent anomalous band migration observed after treatment of the plasmid with $[V_2OX_2(phen)_4]^{2+}$, (2) the stable purple precipitate formed at high complex/DNA ratios that indicates restricted access of the complex to oxygen, (3) the increased T_m for CT DNA exposed to $[V_2OX_2(phen)_4]^{2+}$, and (4) the concentration-dependent band retardation on denaturing gels of 31-mer exposed to $[V_2OX_2(phen)_4]^{2+}$, which persists even after the complex is boiled in a formamide-containing running buffer. The apparent strength of this interaction is consistent with the measured association constant of $>10^5$ M^{-1} with CT DNA. However, the exact nature of the binding—i.e., intercalative, groove binding, electrostatic, or covalent—remains unclear.

Resonance Raman spectroscopy is in principle an ideally suited technique for studying the interaction of metal complexes with biomolecules such as DNA. However, whether because of a lack of suitable chromophores or the inherent fluorescence of many of the metal complexes traditionally used in studying DNA binding, it has not been widely utilized in this area. Nevertheless, we have found it to be a powerful method for studying the interaction of our μ-oxo V(III) dimers with DNA. In particular, RR spectroscopy shows that in frozen aqueous solution, the parent complex $[V_2OCl_2(phen)_4]^{2+}$ undergoes initial aquation, followed by the reaction of the aquated species with the DNA. One possibility is that the aquated complex reacts with the heterocyclic bases of DNA, of which the N-7 of guanine is generally considered to be the most reactive site. However, numerous other interactions could be envisioned. Once the V(III) dimer is bound to the DNA, it is likely that redox takes place, leading to the formation of alkaline-sensitive lesions. Hydrogen peroxide is implicated as a partner in this redox based on the effects of SOD and catalase. Other preliminary results, using analogous μ-oxo V(III) complexes containing a strapped bis-bipyridyl where the chloride ligands are forced to be in a trans rather than cis configuration, show DNA binding but no cleavage activity.[45] Thus, the geometry around the vanadium is critical to the cleavage process but not to the DNA binding. Consistent with this observation is that the trans complex is much less reactive toward oxygen, despite a redox potential similar to that of the active cis isomer.[46]

In conclusion, we have shown that μ-oxo V(III) dimers of the type $[V_2OX_2(phen)_4]^{2+}$ bind strongly to DNA and lead ultimately to its degradation. The exact nature of the cleavage event remains to be elucidated, but it appears to involve oxidative base loss. Further work to clarify the operative chemistry is in progress.

Acknowledgment. This work was supported by Grants AI-1157 (C.J.C.) and E-518 (R.S.C.) from the Robert A. Welch Foundation, R24-RR12253 from the National Center for Research Resources, P01-CA75137 from the National Cancer Institute, and ATP-030 from the Texas Higher Education Coordinating Board, and a grant from the Roy F. and Joan C. Mitte Foundation (R.B.W.).

IC000389R

(45) Grant, C. M.; Stamper, B. J.; Knapp, M. J.; Folting, K.; Huffman, J. C.; Hendrickson, D. N.; Christou, G. *J. Chem. Soc., Dalton Trans.* **1999**, 3399.
(46) Brand, S. G.; Edelstein, N.; Hawkins, C. J.; Shalimoff, G.; Snow, M. R.; Tiekink, E. R. T. *Inorg. Chem.* **1990**, *29*, 434.